Published in final edited form as:
Cytoskeleton (Hoboken). 2010 April ; 67(4): 259–271. doi:10.1002/cm.20443.

Functional roles of VASP phosphorylation in the regulation of chemotaxis and osmotic stress response

Wan-Hsin Lin[*], **Sharon E. Nelson**[#], **Ryan J. Hollingsworth**[#], and **Chang Y. Chung**[#,*]

[#] Department of Pharmacology, Vanderbilt University Medical Center, Nashville, TN 37232-6600

[*] Department of Biological Sciences, School of Art and Science, Vanderbilt University, Nashville, TN 37232-6600

Abstract

VASP plays crucial roles in controlling F-actin-driven processes and growing evidence indicates that VASP function is modulated by phosphorylation at multiple sites. However, the complexity of mammalian system prevents the clear understanding of the role of VASP phosphorylation. In this study, we took advantage of *Dictyostelium* which possesses only one member of the Ena/VASP family to investigate the functional roles of VASP phosphorylation. Our results demonstrated that hyperosmotic stress and cAMP stimulation cause VASP phosphorylation. VASP phosphorylation plays a negative role for the early steps of filopodia/microspikes formation. VASP phosphorylation appears to modulate VASP localization at the membrane cortex and its interactions with WASP and WIPa. Analysis of chemotaxis of cells expressing VASP mutants showed that VASP phosphorylation is required for the establishment of cell polarity under a cAMP gradient.

Keywords

VASP phosphorylation; Actin; Chemotaxis; Cell polarity

Introduction

Vasodilator-stimulated phosphoprotein (VASP) belongs to the Ena/VASP family which also consists of *Drosophila* Enabled (Ena), mammalian Enabled (Mena), and Ena/VASP-like proteins (EVL) (Kwiatkowski et al. 2003). Members of the Ena/VASP family harbor a conserved domain structure with an amino-terminal Ena/VASP homology 1 (EVH1) domain and a carboxyl-terminal Ena/VASP homology 2 (EVH2) domain separated by a more variable proline-rich domain (PRD)(Kwiatkowski et al. 2003). Three conserved motifs are located in the EVH2 domain: a G-actin-binding motif (GAB), a F-actin-binding site (FAB), and a coiled-coil motif (CO) essential for tetramerization (Bachmann et al. 1999). Growing evidence has demonstrated that the Ena/VASP proteins play crucial roles in actin-based cellular processes. Ena/VASP proteins have been shown to localize at dynamic actin structures including focal adhesions, cell-cell contacts, actin stress fibers, leading edges of cells, and tips of filopodia (Lanier et al. 1999; Rottner et al. 1999). Studies on Ena/VASP triple null mice revealed the essential role of the Ena/VASP proteins in endothelial structural integrity and neuritogenesis in the developing cortex (Furman et al. 2007; Kwiatkowski et al. 2007). Ena/VASP proteins are also important in the regulation cell motility. Studies

Address correspondence to: Chang Y. Chung (Chang.Chung@Vanderbilt.edu). 1214 21st Ave. South @ Pierce, 468 Robinson Research Building (MRB I), Nashville, TN 37232-6600; Phone: 615-322-4956; Fax: 615-343-6532.

showed that Ena/VASP proteins are critical in efficient movement of Listeria (Laurent et al. 1999; Smith et al. 1996a) (Loisel et al. 1999; Niebuhr et al. 1997). In contrast, Ena/VASP negatively regulate fibroblast motility by producing longer and less-branched actin filaments in lamellipodia(Bear et al. 2002).

Human VASP contains three phosphorylation sites, and the Ser-157 site within the PRD domain is more conserved among species (Butt et al. 1994). cAMP-dependent protein kinase (PKA), cGMP-dependent protein kinase (PKG), and protein kinase C (PKC) have been demonstrated to directly phosphorylate this position (Butt et al. 1994; Chitaley et al. 2004; Howe et al. 2002; Smolenski et al. 2000). Several physiological stimuli including cell detachment and activation of G protein coupled receptors result in VASP phosphorylation (Profirovic et al. 2005; Smolenski et al. 2000). The effect of VASP phosphorylation on filopodia formation is not quite clear yet. Phosphorylated VASP was reported to play a positive role in the formation of filopodia in neuronal cells (Lin et al. 2007) (Lebrand et al. 2004). In contrast, cells expressing wild-type or nonphosphorylatable mutants of Ena/VASP have similar frequency of filopodia and ruffle formation in spreading fibroblasts (Applewhite et al. 2007). Filopodia have been suggested to function as a probe for cells to sample environmental cues for efficient directional movement. Therefore, we believe that it is important to understand the role of VASP phosphorylation in the ergulation of chemotaxis (Faix et al. 2009). However, the complexity of mammalian cells that possess three Ena/VASP proteins with interchangeable functions and multiple phosphorylation sites makes it very difficult to understand the exact mechanism for how phosphorylation affects their functions during chemotaxis.

Distyostelium discoideum, a single-cell amoebae found growing autonomously on soil bacteria, has been intensely used to study cytoskeleton reorganization and cell chemotaxis. VASP was identified as the sole member of the Ena/VASP family and is required for filopodia formation and chemotaxis in *Dictyostelium* (Han et al. 2002; Schirenbeck et al. 2006). In this study, we used *Dictyostelium* cells that provide a simple system to investigate the role of VASP phosphorylation in controlling cytoskeletal organization and motility during hyperosmotic shock and chemotaxis. Our results indicate that VASP phosphorylation is important for its localization and regulates the interaction with WASP and with WIPa. Additionally, VASP phosphorylation plays a negative role in membrane protrusion, which is crucial for restricted pseudopod extension and efficient chemotaxis.

Materials and Methods

Cell Culture

Dictyostelium cells were cultured axenically in HL5 medium supplemented with 60 U of penicillin and 60 μg of streptomycin per ml. Transformation was by electroporation and selected with G418 containing media. AMPK-AS (AMPK antisense strain HPF456) was kindly provided by Dr. Paul Fisher (La Trobe University, Australia). Other cell strains used in this paper were obtained from Dicty Stock Center.

Molecular Biology and Western blotting

VASP expression constructs were produced by PCR amplification of a *Dictyostelium* cDNA library. The sequences of primers are listed as 5′-gtttggatccatgagtgaaacagcaatttttaa-3′ (forward) and 5′-gtttctcgagatgttgagatgctctgattgctt-3′ (reverse). Then, the construct is subcloned into the pEXP4(+) by using BamHI and XhoI restriction enzyme sites in frame with eYFP at the N-terminus with the flexible linker GSGSG. Using the same strategy, VASP constructs are subcloned into the pDXA-HY vector in frame with the N-terminal His tags. The YFP or His fusion proteins were expressed under the control of the actin-15

promoter. Point mutants were produced by cloning genes into psp72 or pQE30 using the QuikChange site-directed mutagenesis kit (Stratagene, La Jolla, CA) and subcloned into pEXP4(+) or pDXA-HY. All mutants were confirmed by sequence analysis.

Vegetative or 5-hr pulsed cells (~2×10^6 cells) were plated onto 30 mm Petri dishes. After the treatment of hyperosmotic reagents (sorbitol, glucose, NaCl, and urea; 400 mM as final concentration) or cAMP (200nM as final concentration), cells were lysed in ~200 μl lysis buffer (25 mM Tris, (pH7.6), 100 mM NaCl, 1% NP40, 10% Glycerol, 1 mM DTT) in the presence of protease inhibitor cocktail (Sigma, Saint Louis, MO) and phosphatase inhibitors (5 mM NaF, 20 mM sodium pyrophosphate, 40 mM β-glycerophosphate). 20-30 μg of cell lysates or ~3×10ˆ5 cells were suspended in 6× sample buffer and subjected to 8% SDS-PAGE followed by immunoblotting with anti-VASP polyclonal antibody (kindly provided by Dr. Richard Firtel, UCSD, US). Signal was visualized using the ECL plus system (GE healthcare, Buckinghamshire UK).

In vitro pull-down assay and density gradient analysis

Protein expression constructs produced using pGEX-6P1 or pQE30 were transformed into BL21 cells. Cultures were grown to a cell density of OD600 = 0.8 and 0.1 mM IPTG was added to induce protein expression for 4-5 hr at 16 °C (His-VASP and GST-WIPa) or for 40 min at 37 °C (GST-WASP). Proteins were purified according to the manufactures' instructions (GST proteins, Sigma; His proteins, Qiagen). His-tagged proteins and GST-fusion proteins bound to glutathione-conjugated agarose beads were added to 1 ml PBS containing 0.5 % BSA and incubated at 4 °C for 2 hr. The agarose beads were pelleted by centrifugation at 14,000 rpm for 5 min and washed three times with 1 ml 0.1% Tween20-TBS. Bound proteins were then stripped off the beads in 2× sample buffer by boiling for 5 min. Samples were resolved on a 12% SDS-PAGE gel, and proteins were identified via Western analysis using a mouse anti-His tag antibody (Novagen, Germany). Protein signals were visualized using the Odyssey system (LI-COR biosciences, Lincoln, Nebraska).

To perform gradient density analysis, equal amount (50 μg) of His-VASP and GST-WASP were incubated at 4 °C for 2 hr. Immediately, the protein mixtures were overlaid on an Optiprep (Greiner BioOne, Longwood, FL) step gradient (130 μl for each gradient, 20%, 15%, 10%, 5%) and centrifuged in a Beckman SW40Ti rotor (Fullerton, CA) for 18 h at 35,000 rpm at 4°C. Twenty-five μl fractions were collected from the top of tubes and analyzed by SDS-PAGE followed by Coomassie blue staining. Protein bands were quantified using ImageJ software (NIH).

F-actin Staining and Actin Polymerization Assay

Vegetative cells were plated onto flamed coverglass and washed twice with 12 mM Na^+/K^+ phosphate buffer. After 30-60 min synchronization in the phosphate buffer, cells were treated with sorbitol (final 400 mM) for 10 min. Then, cells were fixed and permeabilized in PHEM buffer containing 0.2 % Triton X-100, 0.5 % Glutaraldehyde, 3.7 % Formaldehyde for 10 min. Actin filaments were stained with Texas Red-conjugated phalloidin (6.6 nM, Biotium, Hayward CA) for 1 h. The coverslips were then mounted and viewed under a fluorescence microscope. For actin polymerization assay (Myers et al., 2006), 100 μl of cells were mixed at each time point in lysis buffer (25 mM Tris, pH 7.6, 100 mM NaCl, 1 mM EDTA, 1% NP-40, 10% glycerol, 1 mM DTT, 3 μM phalloidin). Lysates were spun down at 14,000 rpm for 10 min. Pellets were boiled in 2× loading buffer, resolved on 10% SDS-PAGE, blotted onto nitrocellulose, and YFP-WIPa was detected using an anti-GFP antibody.

Chemotaxis Assay

Cells competent to chemotaxis toward cAMP were obtained by pulsing cells with 50 nM cAMP at 6-min intervals for 5 h. Afterwards, cells were plated onto homemade coverglass-bottomed petri dish. Images were taken at 3 s or 6 s intervals by using Metamorph software (Universal Imaging, West Chester, PA). For the chemotaxis assay, a micropipette (WPI) filled with 100μM cAMP was positioned to stimulate cells by using a micromanipulator (Narishige, Tokyo, Japan). Cell path was tracked for 15 min after the micropipette was placed for 5-10 min and analyzed in 6 sec intervals.

Statistics analysis

All data was analyzed by using Prism software (World Headquarters, Irvine, CA). Outliers were defined as the points lie outside the mean ± 2 SD and were not included in the presented data.

Results

VASP phosphorylation by hyperosmotic stress and extracellular cAMP stimulus

VASP is a substrate of PKA, PKG, and PKC (Butt et al. 1994; Chitaley et al. 2004; Howe et al. 2002; Smolenski et al. 2000). In *Dictyostelium*, hyperosmotic shock and extracellular cAMP stimulus have been demonstrated to induce intracellular cAMP and cGMP elevation which are the upstream activators of PKA and PKG, respectively (Ott et al. 2000; Oyama 1996). Therefore, we reasoned that hyperosmotic shock and extracellular cAMP stimulus may result in VASP phosphorylation. To test this, vegetative cells and 5-hr pulsed cells were treated with sorbitol (400 mM) and cAMP (200 nM), respectively. The whole cell lysates from the same amount of cells were subjected to immunoblotting using anti-VASP antibody. VASP phosphorylation is demonstrated by the electrophoretic shift as shown in mammalian cells(Lawrence and Pryzwansky 2001). Sorbitol treatment causes VASP phosphorylation shown as a mobility shift of VASP at the peak of 10-30 minute (Fig. 1A), whereas cAMP induces VASP phosphorylation at the peak of 10-20 seconds after stimulation. We used Image J software to measure the band intensity of phosphorylated VASP which shows slower migration in the gel and total VASP proteins which include unphosphorylated and phosphorylated VASP. Only a small fraction of VASP (<15%) gets phosphorylated upon cAMP stimulation compared to hyperosmotic stress (40-50%). To identify the phosphorylation sites, we first examined potential substrate recognition sites of PKA, PKG, and PKC. We found two putative phosphorylation sites of PKA and PKC located at serine 141 and 351, respectively (Fig. 1B). To identify phosphorylation sites, 6×His-tagged $VASP^{S141A}$, $VASP^{S351A}$, and $VASP^{AA}$ (harboring both S141A and S351A) were expressed in *vasp* null background. $VASP^{S141A}$ completedly abolished the mobility shift, while $VASP^{S351A}$ still showed a shift upon sorbitol treatment. This result indicates that hyperosmotic stress induces VASP phosphorylation at Ser-141 (Fig. 1C). Ser-141 of *Dictyostelium VASP*, the comparable site to the Ser-157 in human VASP, is evolutionally conserved (Kwiatkowski et al. 2003).

Distinct hyperosmotic reagents introduce hyperosmolarity to the cells with varying effects. Sugar and electrolytes are able to cause hyperosmotic shock-induced cell shrinkage. Alternatively, urea does not cause cell shrinkage due to its relatively high membrane-permeability. To further investigate the underlying mechanisms for hyperosmotic shock-induced VASP phosphorylation, cells were treated with glucose, NaCl, sorbitol, or urea (Fig. 1D). In contrast to other hyperosmotic reagents, urea failed to cause VASP phosphorylation, suggesting that hyperosmotic shock-induced VASP phosphorylation is volume-sensitive.

To identify a kinase responsible for VASP phosphroylation, null strains of candidate kinases were used to test for VASP phosphorylation upon hyperosmotic stress. Under hyperosmotic stress, cAMP is elevated due to the inhibition of the hybrid histidine kinase DokA by phosphodiesterase RegA (Ott et al. 2000). The elevation of cAMP activates PKA. On the other hand, cGMP accumulation upon hyperosmotic shock is caused by the activation of soluble guanylyl cyclase (Oyama 1996). To test if sorbitol, through the activation of PKA or cGMP elevation, induces VASP phosphorylation, null strains of PKA catalytic domain (*pka-cat*$^{-}$) and of guanylyl cyclases (sgc/gca^{-}) were tested (Fig. 1E). Comparable level of VASP phosphorylation still occurs in these null cells, indicating sorbitol-induced VASP phosphorylation is not dependent upon PKA and cGMP. The MAP kinase pathway has been known to be the major signaling pathway for the regulation of cellular responses to hyperosmotic shock in organisms ranging from yeast to mammals(Cowan and Storey 2003). In addition, AMP-activated protein kinase (AMPK), which phosphorylates the Thr-278 site of mammalian VASP, can also be activated upon hyperosmotic shock (Blume et al. 2007; Woods et al. 2003). Therefore, VASP phosphorylation was tested in *erkA and erkB* null cells and in an AMPK antisense strain (Fig. 1E). Neither ERKs nor AMPK is responsible for sorbitol-induced VASP phosphorylation. It has been demonstrated that SAPKα is important for cellular resistance to osmotic stress and that SAPKα mutants affect cellular processes requiring proper regulation of the actin cytoskeleton, including cell motility, morphogenesis, cytokinesis, and cell adhesion(Sun et al. 2003a). VASP still gets phosphorylated in *sapkA*$^{-}$cells upon osmotic stress. Thus, the identity of the kinase(s) which can cause VASP phosphorylation remains unknown.

VASP phosphorylation plays a negative role in filopodia formation

To assess the functional role of VASP phosphorylation in *Dictyostelium*, we generated cells expressing YFP-tagged VASP, an unphosphorylatable (Ser^{141} to Ala) mutant, or a phosphomimetic (Ser to Asp) mutant (hereafter referred as SA or SD, respectively) in the *vasp* null background. YFP-VASP and mutant proteins were detected by immunoblotting at comparable expression levels to endogenous VASP (Fig. 2A). Ena/VASP proteins have been known to drive the processes of filopodia formation (Dent et al. 2007;Han et al. 2002;Schirenbeck et al. 2006). Similar to mammalian VASP, *Dictyostelium* VASP enriches at the tips of filopodia, and the *vasp* null cells fail to generate filopodia (Han et al. 2002;Schirenbeck et al. 2006). However, the role of VASP phosphorylation in filopodia formation remains unclear. To answer this question, cells expressing VASP phosphorylation mutants were stained with phalloidin to visualize F-actin organization(Fig. 2B). Since microspikes and filopodia both contain parallel actin bundles and may be related to each other (Svitkina et al. 2003), we termed these finger-like protrusions in the cells as filopodia/microspikes in this study. We measured the number and the length of filopodia/microspikes in individual cells from different strains (Fig. 2C and D). Cells expressing wild-type VASP protruded comparable number and length of filopodia/microspikes (average number per cell 14.5 ± 5) to KAx3 strain (average number per cell 14.3 ± 3). Intriguingly, SA and SD mutations on VASP exhibited different effects on filopodia/microspikes formation. Expression of SA-VASP fully rescued (average number per cell 13.6 ± 6.7) the defect of filopodia/microspikes formation of *vasp* null cells. In contrast, expression of SD-VASP only partially rescued filopodia formation (average number per cell 10.0 ± 5.1). Nevertheless, there is no significant difference in the length of filopodia/microspikes protrusion among these cells. The localization of VASP at the tips of filopodia is not also affected by its phosphorylation.

VASP Phosphorylation determines its subcellular localization

To determine if VASP phosphorylation affects its localization, we examined the association of these VASP mutants with the detergent insoluble cytoskeleton/membrane fraction (Fig.

3A). Vegetative stage cells were treated with 0.2 M sorbitol and lysed with lysis buffer (25 mM Tris, pH 7.6, 100 mM NaCl, 1 mM EDTA, 1% NP-40, 10% glycerol, 1 mM DTT). Detergent-insoluble fraction (DIF) was pelleted by spinning lysate at 18,000 rpm. The association of YFP-VASP or –SA-VASP, or -SD-VASP associated with the DIF was detected by western blot. As shown in Fig. 3A, all three showed reduced association with the DIF initially after sorbitol treatment. However, YFP-SA-VASP showed the recovery in DIF-association at 5 min after sorbitol treatment. In contrast, the association YFP-VASP and SD-VASP appears to be further reduced at 5 min. To examine changes in F-actin polymerization in DIF, DIF was run on PAGE gels and intensities of actin bands at different time points after sorbitol treatment were quantified (Fig. 3B). Similar to VASP or mutant, F-actin polymerization in all three cells was reduced at early time points. The reduction of F-actin polymerization was minimal in cells expressing YFP-SA-VASP and exhibited a recovery up to normal level at 5 min while YFP-VASP and YFP-SD-VASP showed further reduction of F-actin polymerization at 5 min. Differential localization of SA- and SD-VASP in DIF indicates that the phosphorylation of VASP might have an important role for its localization. To examine subcellular localization of YFP-VASP and F-actin organization, cells were stained with phalloidin (Fig. 3C). In response to hyperosmotic shock with sorbitol, all three cells appear to form puntae of YFP-VASP or mutants. As mammalian VASP has been reported to form tetramer(Bachmann et al. 1999), it is plausible that *Dictyostelium* VASP also forms a tetramer. These punctate stainings were also observed by the immunostaining of endogenous VASP (data not shown). After 5 min of sorbitol treatment, cells expressing YFP-VASP showed F-actin staining along the cortical membrane and colocalization of YFP-VASP and F-actin was hardly observed. F-actin organization in cells expressing YFP-SD-VASP was different, showing patches of F-actin. However, lack of significant colocalization of F-actin with YFP-SD-VASP was similar to YFP-VASP. F-actin staining of cells expressing YFP-SA-VASP clearly showed a significant colocalization with YFP-SA-VASP. This result suggests that VASP phosphorylation negatively regulate the localization of VASP with F-actin at the membrane cortex.

VASP is required for cell size change upon hyperosmotic stress

To determine the functional role of differential localization of VASP mutants, we examined if VASP or VASP phosphorylation is required for cell size change upon hyperosmotic stress. Vegetative cells were stimulated with 0.2 M sorbitol and fixed at different time points to examine the change of cell size. Wild type cells showed 37% reduction of cell size (measured compared to untreated cells at 2 min and maintained the same level of shrinkage at 5 min (Fig. 3D). In contrast, *vasp* null cells exhibited delayed reduction of cell size, showing less than 20% reduction at 2 min but further reduction of cell size comparable to the wild type cells at 5 min. This result suggests that VASP might be important for early stage of cell shrinkage induced by hyperosmotic shock. Expression of YFP-VASP rescued the defect of null cells or showed even further reduction of cell size than wild type cells. Expression of SA-VASP or SD-VASP did not cause significant cell shrinkage at 2 min after sorbitol treatment. However, SA-VASP and SD-VASP cells showed a clear difference at 5 min after sorbitol treatment. SD-VASP cells exhibited significant reduction of cell size at 5 min whereas SA-VASP cells showed recovery of cell size to the level of untreated cells. These results suggest that cells might need combination of both phosphorylated and unphosphroylated VASP at different stage to regulate the organization of F-actin for the reduction and restoration of cell size upon hyperosmotic stress.

cAMP for the regulation of has been shown to induce cAMP receptor activation followed by phosphatydylinositol-3 phosphates ($PI(3,4,5)P_3$/$PI(3,4)P_2$) production and the cortical translocation of proteins, including VASP (Chung and Firtel 2002; Han et al. 2002). Nevertheless, it is unclear whether the translocation of VASP in response to cAMP requires

phosphorylation. To determine the importance of VASP phosphorylation in the localization VASP, we used time-lapse imaging to examine the localization of VASP mutants. As previously reported (Han et al. 2002), VASP translocates to the cortical membrane with maximum intensity at 6 seconds (Fig. 4A). However, the mutation at Ser-141 significantly diminishes VASP translocation. While YFP-SA-VASP exhibits little translocation to the cortex, YFP-SD-VASP shows some level of translocation even though it was less than YFP-VASP. This result again shows that VASP phosphorylation affects its localization. We also examined the association of these VASP mutants and F-actin polymerization in DIF (Fig. 4B and C). YFP-VASP showed two peaks of DIF association at 10 sec and 60 sec after cAMP stimulation. YFP-SD-VASP showed similar changes. In contrast, YFP-SA-VASP exhibited weaker first peak but much higher and long-lasting second peak of DIF association at 60-80 sec. YFP-SA-VASP cells also showed a strong second peak of F-actin at 80 sec while YFP-VASP or YFP-SD-VASP cells exhibited a small or no peak at 60 sec, respectively. We examined the colocalization of VASP mutants and F-actin at 60 sec after cAMP stimulation. YFP-VASP showed colocalization at the cortical membrane of pseudopods and YFP-SA-VASP exhibited much greater colocalization along cortical membrane. However, YFP-SD-VASP showed minimal colocalization with F-actin, consistent with DIF association data.

VASP phosphorylation affects its binding affinity to WASP and WIPa

VASP has been suggested to interact with the proline rich domain of WASP, presumably via its EVH1 domain (Castellano et al. 2001). In addition, the EVH1 domain of VASP determines its interaction with WASP interacting protein (WIP) (Myers et al. 2006; Rong and Vihinen 2000; Volkman et al. 2002). Since both WASP and WIP are important regulators of F-actin organization, we reasoned that VASP phophorylation might regulate interactions of VASP with WASP or WIPa. We performed GST-pulldown experiments with GST-WIPa- or GST-WASP-bound glutathione beads and recombinant wild type(WT)- or SD-VASP proteins with 6×His tags. Wild-type VASP showed minimal binding to WIPa in the pull-down assays. However, SD-VASP showed higher affinity to WIPa whereas its interaction with GST-WASP was significantly weaker than the wild type (Fig. 5A). To further verify the effect of VASP phosphorylation on the interaction between VASP and WASP, we performed density gradient centrifugation analysis. GST-WASP and His-VASP proteins were incubated and then the mixture was subjected to centrifugation on the Optiprep density gradient (5-20%). Equal volume of samples were taken from the gradient and resolved on SDS-PAGE gels. His-VASP and GST-WASP proteins were visualized by Coomassie blue staining and band intensities were quantified. As shown in Figure 5B, in the absence of GST-WASP proteins, most of VASP proteins were distributed in fractions 8-13. Presence of GST-WASP in the gradient causes shift of VASP peak to fraction 20, indicating the physical interaction of VASP and WASP. In contrast, the presence of GST-WASP does not cause significant shift of SD-VASP peak to higher fractions (Fig. 5B). Accordingly, we see more WASP proteins shift to the same fraction with VASP, but not with SD-VASP. Taken together, VASP phosphorylation appears to determine its affinity for the interaction with WASP or WIPa. Phosphorylation of VASP abolishes its interaction with WASP while phosphorylation contributes to the binding to WIPa with higher affinity.

Phosphorylated VASP determines directional efficiency and generation of cell polarity during chemotaxis

Membrane protrusions such as filopodia/microspikes and pseudopods function as antenna for cells to explore the environmental cues to guide cell movement. Thus, one might imagine that VASP phophorylation upon chemoattractant stimulation would have an important role for the regulation of chemotaxis. In neutrophils, chemoattractant fMLP induces VASP phosphorylation and cell migration (Eckert and Jones 2007). However, the

exact role of VASP phosphorylation in the regulation of chemotaxis is still unknown. In order to examine if VASP phosphorylation affects directional movement, we performed a random motility assay and micropipette chemotaxis assay combined with time-lapse imaging. In the absence of a cAMP chemoattractant gradient, the KAx3 strain and cells expressing VASP in *vasp* null background exhibited faster movement than *vasp* null cells (Fig. 6A), indicating the involvement of VASP in controlling random motility. However, expression of SA- and SD-VASP failed to fully rescue the motility defects of the null cells. These data suggest that phosphorylation of VASP plays a role in the regulation of random motility. In a chemotaxis assay, both KAx3 and VASP/*vasp*$^-$ cells showed quick and straight movement up the gradient (Fig. 6B and C). This movement is led by the predominant pseudopod at the leading edges while lifespan of the lateral or rear pseudopods are usually short (Movie S1. and S3.). In contrast, *vasp* null cells did not exhibit a strong chemotaxis response, leading to slower cell speed and less directional efficiency. Some of the null cells appeared to be round or stayed at their initial positions for a while before they started to move while some cells exhibited better directional movement even though they move at a slower speed than VASP/*vasp*$^-$ cells (Movie S2). SD-VASP/*vasp*$^-$ cells, in general, exhibited similar chemotactic responses to VASP/*vasp*$^-$ cells (Movie S5). SA-VASP/*vasp*$^-$ cells usually possess bifurcated pseudopods in the direction of the gradient or frequently extend pseudopods even in the lateral directions (Movie S4). This result indicates that SA-VASP/*vasp*$^-$ cells has a significant defect in the suppression of lateral or rear pseudopods, causing lower directional efficiency during chemotaxis (Fig. 6D). Surprisingly, the speed of SA-VASP/*vasp*$^-$ cells was not greatly hampered compared to VASP/*vasp*$^-$ cells even though they exhibit directionality defects (Fig. 6C).

One notable difference of SA-VASP/*vasp*$^-$ cells from wild-type or VASP/*vasp*$^-$ cells was lack of polarity. To examine if VASP phosphorylation affects cAMP gradient-induced cell polarization, we measured the polarity of the cells right after and 20 min after the micropipette is placed (Fig. 7A and B). *vasp* null cells cringe and become more rounded up than other cells upon the placement of the micropipette, whereas wild type cells usually cringe and then start to extend pseudopods and elongate the cell body over time. This defect of *vasp*$^-$ cells was rescued by expressing VASP or SD-VASP. These cells become more polarized and actively migrate after 20 min. However, SA-VASP/*vasp*$^-$ cells exhibit less polarized morphology than VASP/*vasp*$^-$ and SD-VASP/*vasp*$^-$ cells, presumably due to lack of a dominant leading edge protrusion and the multiple protrusions around the cell. F-actin staining of KAx3 cells showed accumulation of F-actin staining at the leading and trailing edge that is absent in *vasp* null cells. Expression of VASP or SD-VASP in *vasp* null cells rescues polararized F-actin organization. However, SA-VASP expressing cells lacked polarity of F-actin organization as they did not show prominent F-actin staining at a specific area. They instead showed patches of small F-actin enrichment at the cortex that presumably are sites of pseudopod formation. Taken together, phosphorylated VASP is required for the suppression of lateral or rear pseudopods and the establishment of cell polarity in order to achieve efficient chemotaxis.

Discussion

The coordination of the actin cytoskeleton rearrangement regulates a diverse variety of cellular processes, such as cell-shape change, membrane protrusion, and cell movement. Accumulation of F-actin to membrane cortex by the reorganization of the actin cytoskeleton plays an important role in withstanding hyperosmotic environments (Di Ciano et al. 2002; Rivero et al. 1996) and also mediates membrane protrusion during cell migration (Lambrechts et al. 2008; Mattila and Lappalainen 2008). VASP has been demonstrated to regulate cell-morphology change, filopodia formation, cell motility, and chemotaxis (Bear et al. 2000; Han et al. 2002; Hauser et al. 1999; Schirenbeck et al. 2006). However, it is not

clear how VASP phosphorylation regulates these events. In this study, we demonstrated that VASP phosphorylation plays a negative role in filopodia/microspikes protrusion. Additionally, we showed that the regulation of VASP phosphorylation is important for its localization to the membrane cortex and interaction with WASP and WIPa. Moreover, VASP phophorylation is required for the establishment of cell polarity during chemotaxis.

VASP was first identified as a substrate of PKA and PKG which are regulated by cyclic nucleotides (Reinhard et al. 1992). In *Dictyostelium*, cyclic nucleotides have been demonstrated to govern chemotaxis and development, and are also essential for cellular response to hyperosmotic shock (Chung and Firtel 2002; Mahadeo and Parent 2006; Ott et al. 2000; Oyama 1996). Our data indicates that VASP phosphorylation at Ser-141 can be induced by hyperosmotic shock (sorbitol) and kinetics of VASP phosphorylation is parallel to that of intracellular cAMP concentration, suggesting PKA would be a good candidate for the kinase phosphorylating Ser-141. However, VASP was still phosphorylated in *pka/cat*$^{-}$ null cells, effectively ruling out PKA as a potential kinase for VASP. Experiments with null strains also suggested that VASP phosphorylation is independent of cyclic nucleotides (Fig. 2). Lack of VASP phosphorylation when cells were treated with cell-permeable cAMP and cGMP derivatives (8-Br-cAMP/8-Br-cGMP) (data not shown) and lack of VASP phosphorylation in *sgc/gca* null cells support the independence of VASP phosphorylation from cyclic nucleotides. To date, several kinases have been reported to be activated upon sorbitol treatment in *Dictyostelium*. A Stress-activated protein kinase (SAPKα) has been demonstrated to be important for cells to withstand hyperosmotic stress (Sun et al. 2003b). In addition, a stress response kinase (KrsA) has also been activated upon sorbitol treatment and is responsible for cAMP elevation in this condition (Muramoto et al. 2007). In this study, we ruled out the SAPKα as a kinase for VASP phosphorylation. Several pieces of evidence direct that calcium/calmodulin-dependent protein kinase II (CaM kinase II) may regulate VASP phosphorylation upon hyperosmotic shock. DdVASP sequences (RXXST(V)) flanking Ser-141 matches the consensus phosphorylation sites of CaMKII (Pearson et al. 1985). The solely identified CaMKII homolog in *Dictyostelium* is myosin light chain kinase-A (MLCK-A) (Smith et al. 1996b). MLCK-A has been demonstrated to phosphorylate Kemptide (LRRASLG) (Tokumitsu et al. 2004), which correspond to the RXXS motif at VASP-Ser141. Therefore, it is important to test if MLCK-A or other putative CaM kinases are responsible for sorbitol-induced VASP phosphorylation.

We demonstrated that the expression of phosphomimetic VASP in *vasp* null cells decreases the number of filopodia/microspikes while it does not affect the length of filopodia/microspikes. This result suggests that VASP phosphorylation might have a negative effect on filopodia formation. Filopodia formation comprises a series of complex processes including initiation, formation/elongation, and stabilization. A de novo filament nucleation model and a convergent elongation model have been proposed to explain the formation of filopodia (Medalia et al. 2007; Svitkina et al. 2003). First, formin-nucleated F-actin barbed ends at the plasma membrane converge in order to initiate the whole process. Second, the elongation of protected actin filaments provides the propelling force for membrane deformation. VASP has been shown to localize at the tip of filopodia (Lanier et al. 1999) and plays a critical role in filopodia formation in many different systems, including *Dictyostelium* (Han et al. 2002; Lebrand et al. 2004; Pula et al. 2006). Several lines of evidence suggest that phosphorylation may regulate VASP function in filopodia formation. In cultured primary hippocampal neurons, Netrin-1-induced filopodia formation depends on Mena and coincides with increased Mena phosphorylation (Lebrand et al. 2004). Consistent with this observation, overexpression of the Ena/VASP proteins augments Syndecan-2/PKA-dependent filopodia protrusion in the same system (Lin et al. 2007). In our previous study(Myers et al. 2006), we showed that the average steady state number of filopodia/microspikes per cell was significantly increased in cells overexpressing wild-type WIPa, and

WIPa promotes the elongation of actin filaments. VASP phosphorylation appears to increase the affinity of VASP-WIPa interaction as shown in this study. It is possible that increased VASP-WIPa interaction might hinder binding site(s) to F-actin or cause sequestration of VASP or WIPa, causing less efficient initiation of filopodia/microspikes formation.

In our study, we demonstrated that the phosphomimetic mutation causes less VASP localization and F-actin polymerization in the detergent insoluble cytoskeleton fraction and cells expressing nonphosphorylatable SA-VASP exhibited higher level of VASP localization and F-actin polymerization upon sorbitol stimulation. These results suggest that VASP phosphorylation is important for its cortical localization and, in turn, the regulation of F-actin polymerization. The ability of cells expressing YFP-SA-VASP to recover their cell size under hyperosmotic stress might be due to the higher F-actin polymerization. As SA-VASP also showed significant enrichment in the cytoskeleton fraction at later time point upon either cAMP stimulation and this enrichment appears to be correlated with higher F-actin polymerization, VASP might need to be dephosphorylated to be recruited to F-actin at this stage. Higher level of colocalization of SA-VASP with F-actin in these cells is also consisitent with this idea. However, it should be noted that phosphomutants of Mena localized in a subcellular pattern indistinguishable from wild-type EGFP-Mena even though they can't comlement loss of Ena/VASP function(Loureiro et al. 2002).

Wild-type VASP showed minimal binding to WIPa in the pull-down assays. However, SD-VASP showed higher affinity to WIPa whereas its interaction with GST-WASP was significantly weaker than the wild type. It is also intriguing possibility that differential binding of VASP with WIPa or WASP leads different organization of F-actin (i.e. filopodia vs lamellipodia). In the previous study, we demonstrated that WIPa translocates to the cortical membrane upon cAMP stimulation(Myers et al. 2006) and sorbitol treatment (W.L. and C.Y.C, unpublished data). As we showed that phosphorylation of VASP increases its binding affinity to WIPa, it is likely that the interaction between VASP and WIPa plays an important role for the localization of VASP to a specific area of cortical membrane. Upon hyperosmotic stress, VASP may be recruited to the cortex by additional interactions with other proteins, such as F-actin or SH3 domain containing proteins. Biochemical experiments have shown that F-actin is a common interacting partner for both unphosphorylated and phosphorylated VASP(Barzik et al. 2005; Harbeck et al. 2000; Lambrechts et al. 2000; Laurent et al. 1999). Alternatively, unphosphorylated VASP may be recruited by proteins containing SH3 domain(s). Proteins with SH3 domain(s) including αII-Spectrin, Abl, and nSrc have been demonstrated to specifically interact with VASP, and phosphorylation abolishes the interaction between VASP and these proteins(Benz et al. 2008; Lambrechts et al. 2000).

In this current study, we have found that VASP is required for random motility since *vasp* null cells exhibit slow speed of random movement. The phosphorylation status of VASP might be involved in the regulation of random motility since both SA and SD VASP cannot rescue the null phenotype. Different from our observation, the first study in *Dictyostelium* VASP does not reveal the effect of VASP in random movement (Han et al. 2002). This discrepancy is most likely due to the different cell stage when the random movement was examined. In Han's work, cells were grown with bacteria and then starved for 1 hr, whereas, in our study, 5-hr pulsed cells were used in order to compare the random movement with cell chemotaxis. In response to cAMP gradient, *vasp* null cells move with slower speed and less directional determination compared with KAx3 and VASP-expressing cells, consistent with the previous study (Han et al. 2002). More interestingly, the distinct phenotypes of SA and SD cells indicate the importance of VASP phosphorylation for the regulation of efficient chemotaxis. SA-VASP cells lack not only polarity but ability to block or retract lateral and rear protrusions, leading to frequent and persistent movement towards wrong directions.

This results in lower directional efficiency. Failure to suppress lateral pseudopods has been described in several *Dictyostelium* mutants including *pten*- and this defect has been related to failure of actin and myosin II to cortically localize in response to chemoattractant(Wessels et al. 2007). Cortical F-actin might fail to localize in SA-VASP cells, leading to inability to control lateral pseudopods. Surprisingly, even though SA cells fail to perform many stereotypical characteristics of cell chemotaxis, they exhibit faster speed than VASP and SD-VASP cells. Unphosphorylated VASP and phosphorylated VASP play opposite roles in cell polarity and restricted pseudopod extension. Therefore, when there is no expression of VASP in the cells, we do not see either rampant pseudopod extension around the cells like SA-VASP cells or well-established polarity like SD-VASP cells. Second, SA cells fail to establish cell polarity under the cAMP gradient, presumably due to the lack of precise control on the translocation of SA-VASP to the cell cortex. Highly controlled pseudopod extension has been considered as a prerequisite hallmark of chemotactic response (Weber 2006). Cells have to protrude predominant pseudopods at the leading edge and lateral or rear pseudopods have to be retracted for not distracting the directionality of cell movement. VASP has been clearly demonstrated to induce actin polymerization *in vitro*, and its phosphorylation diminishes this effect (Barzik et al. 2005; Harbeck et al. 2000; Lambrechts et al. 2000). Unphosphorylatable VASP might cause uncontrolled pseudopods formation around the cell due to the lack of regulation by VASP phosphorylation. Interestingly, we found some SA cells move linearly toward a cAMP gradient (data not shown). However, these cells still exhibit rampant pseudopods and are less polarized. Therefore, there may be other mechanisms present responsible for chemotaxis without the requirement of confined pseudopod extensions and cell polarity. Combined with the results from SA and SD cells, we clearly demonstrated the functional roles of VASP phosphorylation during chemotaxis.

Supplementary Material

Refer to Web version on PubMed Central for supplementary material.

Acknowledgments

The authors want to deeply thank to Scott Gruver for valuable discussion and suggestions during the progress of this study and his critical reading of this manuscript. We are indebted to Dr. Rick Firtel at UCSD for providing VASP antibody. Also, we thank Yunxiang Zhao for the assistance of data analysis. This work was supported by grants from National Institute of Health (GM68097 to C.Y.C.) and American Heart Association (0655167B to C.Y.C).

References

Applewhite DA, Barzik M, Kojima S, Svitkina TM, Gertler FB, Borisy GG. Ena/VASP proteins have an anti-capping independent function in filopodia formation. Mol Biol Cell. 2007; 18(7):2579–91. [PubMed: 17475772]

Bachmann C, Fischer L, Walter U, Reinhard M. The EVH2 domain of the vasodilator-stimulated phosphoprotein mediates tetramerization, F-actin binding, and actin bundle formation. J Biol Chem. 1999; 274(33):23549–57. [PubMed: 10438535]

Barzik M, Kotova TI, Higgs HN, Hazelwood L, Hanein D, Gertler FB, Schafer DA. Ena/VASP proteins enhance actin polymerization in the presence of barbed end capping proteins. J Biol Chem. 2005; 280(31):28653–62. [PubMed: 15939738]

Bear JE, Loureiro JJ, Libova I, Fassler R, Wehland J, Gertler FB. Negative regulation of fibroblast motility by Ena/VASP proteins. Cell. 2000; 101(7):717–28. [PubMed: 10892743]

Bear JE, Svitkina TM, Krause M, Schafer DA, Loureiro JJ, Strasser GA, Maly IV, Chaga OY, Cooper JA, Borisy GG, et al. Antagonism between Ena/VASP proteins and actin filament capping regulates fibroblast motility. Cell. 2002; 109(4):509–21. [PubMed: 12086607]

Benz PM, Blume C, Moebius J, Oschatz C, Schuh K, Sickmann A, Walter U, Feller SM, Renne T. Cytoskeleton assembly at endothelial cell-cell contacts is regulated by alphaII-spectrin-VASP complexes. J Cell Biol. 2008; 180(1):205–19. [PubMed: 18195108]

Blume C, Benz PM, Walter U, Ha J, Kemp BE, Renne T. AMP-activated protein kinase impairs endothelial actin cytoskeleton assembly by phosphorylating vasodilator-stimulated phosphoprotein. J Biol Chem. 2007; 282(7):4601–12. [PubMed: 17082196]

Butt E, Abel K, Krieger M, Palm D, Hoppe V, Hoppe J, Walter U. cAMP- and cGMP-dependent protein kinase phosphorylation sites of the focal adhesion vasodilator-stimulated phosphoprotein (VASP) in vitro and in intact human platelets. J Biol Chem. 1994; 269(20):14509–17. [PubMed: 8182057]

Castellano F, Le Clainche C, Patin D, Carlier MF, Chavrier P. A WASp-VASP complex regulates actin polymerization at the plasma membrane. Embo J. 2001; 20(20):5603–14. [PubMed: 11598004]

Chitaley K, Chen L, Galler A, Walter U, Daum G, Clowes AW. Vasodilator-stimulated phosphoprotein is a substrate for protein kinase C. FEBS Lett. 2004; 556(1-3):211–5. [PubMed: 14706852]

Chung CY, Firtel RA. Signaling pathways at the leading edge of chemotaxing cells. J Muscle Res Cell Motil. 2002; 23(7-8):773–9. [PubMed: 12952075]

Cowan KJ, Storey KB. Mitogen-activated protein kinases: new signaling pathways functioning in cellular responses to environmental stress. J Exp Biol. 2003; 206(7):1107–1115. [PubMed: 12604570]

Dent EW, Kwiatkowski AV, Mebane LM, Philippar U, Barzik M, Rubinson DA, Gupton S, Van Veen JE, Furman C, Zhang J, et al. Filopodia are required for cortical neurite initiation. Nat Cell Biol. 2007; 9(12):1347–59. [PubMed: 18026093]

Di Ciano C, Nie Z, Szaszi K, Lewis A, Uruno T, Zhan X, Rotstein OD, Mak A, Kapus A. Osmotic stress-induced remodeling of the cortical cytoskeleton. Am J Physiol Cell Physiol. 2002; 283(3):C850–65. [PubMed: 12176742]

Eckert RE, Jones SL. Regulation of VASP serine 157 phosphorylation in human neutrophils after stimulation by a chemoattractant. J Leukoc Biol. 2007; 82(5):1311–21. [PubMed: 17684042]

Faix J, Breitsprecher D, Stradal TEB, Rottner K. Filopodia: Complex models for simple rods. Intl J Biochem Cell Biol. 2009; 41:1656–1664.

Furman C, Sieminski AL, Kwiatkowski AV, Rubinson DA, Vasile E, Bronson RT, Fassler R, Gertler FB. Ena/VASP is required for endothelial barrier function in vivo. J Cell Biol. 2007; 179(4):761–75. [PubMed: 17998398]

Han YH, Chung CY, Wessels D, Stephens S, Titus MA, Soll DR, Firtel RA. Requirement of a vasodilator-stimulated phosphoprotein family member for cell adhesion, the formation of filopodia, and chemotaxis in dictyostelium. J Biol Chem. 2002; 277(51):49877–87. [PubMed: 12388544]

Harbeck B, Huttelmaier S, Schluter K, Jockusch BM, Illenberger S. Phosphorylation of the vasodilator-stimulated phosphoprotein regulates its interaction with actin. J Biol Chem. 2000; 275(40):30817–25. [PubMed: 10882740]

Hauser W, Knobeloch KP, Eigenthaler M, Gambaryan S, Krenn V, Geiger J, Glazova M, Rohde E, Horak I, Walter U, et al. Megakaryocyte hyperplasia and enhanced agonist-induced platelet activation in vasodilator-stimulated phosphoprotein knockout mice. Proc Natl Acad Sci U S A. 1999; 96(14):8120–5. [PubMed: 10393958]

Howe AK, Hogan BP, Juliano RL. Regulation of vasodilator-stimulated phosphoprotein phosphorylation and interaction with Abl by protein kinase A and cell adhesion. J Biol Chem. 2002; 277(41):38121–6. [PubMed: 12087107]

Kwiatkowski AV, Gertler FB, Loureiro JJ. Function and regulation of Ena/VASP proteins. Trends Cell Biol. 2003; 13(7):386–92. [PubMed: 12837609]

Kwiatkowski AV, Rubinson DA, Dent EW, Edward van Veen J, Leslie JD, Zhang J, Mebane LM, Philippar U, Pinheiro EM, Burds AA, et al. Ena/VASP Is Required for neuritogenesis in the developing cortex. Neuron. 2007; 56(3):441–55. [PubMed: 17988629]

Lambrechts A, Gevaert K, Cossart P, Vandekerckhove J, Van Troys M. Listeria comet tails: the actin-based motility machinery at work. Trends Cell Biol. 2008; 18(5):220–7. [PubMed: 18396046]

Lambrechts A, Kwiatkowski AV, Lanier LM, Bear JE, Vandekerckhove J, Ampe C, Gertler FB. cAMP-dependent protein kinase phosphorylation of EVL, a Mena/VASP relative, regulates its interaction with actin and SH3 domains. J Biol Chem. 2000; 275(46):36143–51. [PubMed: 10945997]

Lanier LM, Gates MA, Witke W, Menzies AS, Wehman AM, Macklis JD, Kwiatkowski D, Soriano P, Gertler FB. Mena is required for neurulation and commissure formation. Neuron. 1999; 22(2): 313–25. [PubMed: 10069337]

Laurent V, Loisel TP, Harbeck B, Wehman A, Grobe L, Jockusch BM, Wehland J, Gertler FB, Carlier MF. Role of proteins of the Ena/VASP family in actin-based motility of Listeria monocytogenes. J Cell Biol. 1999; 144(6):1245–58. [PubMed: 10087267]

Lawrence DW, Pryzwansky KB. The vasodilator-stimulated phosphoprotein is regulated by cyclic GMP-dependent protein kinase during neutrophil spreading. J Immunol. 2001; 166(9):5550–6. [PubMed: 11313394]

Lebrand C, Dent EW, Strasser GA, Lanier LM, Krause M, Svitkina TM, Borisy GG, Gertler FB. Critical role of Ena/VASP proteins for filopodia formation in neurons and in function downstream of netrin-1. Neuron. 2004; 42(1):37–49. [PubMed: 15066263]

Lin YL, Lei YT, Hong CJ, Hsueh YP. Syndecan-2 induces filopodia and dendritic spine formation via the neurofibromin-PKA-Ena/VASP pathway. J Cell Biol. 2007; 177(5):829–41. [PubMed: 17548511]

Loisel TP, Boujemaa R, Pantaloni D, Carlier MF. Reconstitution of actin-based motility of Listeria and Shigella using pure proteins. Nature. 1999; 401(6753):613–6. [PubMed: 10524632]

Loureiro JJ, Rubinson DA, Bear JE, Baltus GA, Kwiatkowski AV, Gertler FB. Critical Roles of Phosphorylation and Actin Binding Motifs, but Not the Central Proline-rich Region, for Ena/Vasodilator-stimulated Phosphoprotein (VASP) Function during Cell Migration. Mol Biol Cell. 2002; 13(7):2533–2546. [PubMed: 12134088]

Mahadeo DC, Parent CA. Signal relay during the life cycle of Dictyostelium. Curr Top Dev Biol. 2006; 73:115–40. [PubMed: 16782457]

Mattila PK, Lappalainen P. Filopodia: molecular architecture and cellular functions. Nat Rev Mol Cell Biol. 2008; 9(6):446–54. [PubMed: 18464790]

Medalia O, Beck M, Ecke M, Weber I, Neujahr R, Baumeister W, Gerisch G. Organization of actin networks in intact filopodia. Curr Biol. 2007; 17(1):79–84. [PubMed: 17208190]

Muramoto T, Kuwayama H, Kobayashi K, Urushihara H. A stress response kinase, KrsA, controls cAMP relay during the early development of Dictyostelium discoideum. Dev Biol. 2007; 305(1): 77–89. [PubMed: 17362909]

Myers SA, Leeper LR, Chung CY. WASP-interacting protein (WIPa) is important for actin filament elongation and prompt pseudopod formation in response to a dynamic chemoattractant gradient. Mol Biol Cell. 2006; 17:4564–4575. [PubMed: 16899512]

Niebuhr K, Ebel F, Frank R, Reinhard M, Domann E, Carl UD, Walter U, Gertler FB, Wehland J, Chakraborty T. A novel proline-rich motif present in ActA of Listeria monocytogenes and cytoskeletal proteins is the ligand for the EVH1 domain, a protein module present in the Ena/VASP family. Embo J. 1997; 16(17):5433–44. [PubMed: 9312002]

Ott A, Oehme F, Keller H, Schuster SC. Osmotic stress response in Dictyostelium is mediated by cAMP. Embo J. 2000; 19(21):5782–92. [PubMed: 11060029]

Oyama M. cGMP accumulation induced by hypertonic stress in Dictyostelium discoideum. J Biol Chem. 1996; 271(10):5574–9. [PubMed: 8621417]

Pearson RB, Woodgett JR, Cohen P, Kemp BE. Substrate specificity of a multifunctional calmodulin-dependent protein kinase. J Biol Chem. 1985; 260(27):14471–6. [PubMed: 4055784]

Profirovic J, Gorovoy M, Niu J, Pavlovic S, Voyno-Yasenetskaya T. A novel mechanism of G protein-dependent phosphorylation of vasodilator-stimulated phosphoprotein. J Biol Chem. 2005; 280(38): 32866–76. [PubMed: 16046415]

Pula G, Schuh K, Nakayama K, Nakayama KI, Walter U, Poole AW. PKCdelta regulates collagen-induced platelet aggregation through inhibition of VASP-mediated filopodia formation. Blood. 2006; 108(13):4035–44. [PubMed: 16940418]

Reinhard M, Halbrugge M, Scheer U, Wiegand C, Jockusch BM, Walter U. The 46/50 kDa phosphoprotein VASP purified from human platelets is a novel protein associated with actin filaments and focal contacts. Embo J. 1992; 11(6):2063–70. [PubMed: 1318192]

Rivero F, Koppel B, Peracino B, Bozzaro S, Siegert F, Weijer CJ, Schleicher M, Albrecht R, Noegel AA. The role of the cortical cytoskeleton: F-actin crosslinking proteins protect against osmotic stress, ensure cell size, cell shape and motility, and contribute to phagocytosis and development. J Cell Sci. 1996; 109(Pt 11):2679–91. [PubMed: 8937986]

Rong SB, Vihinen M. Structural basis of Wiskott-Aldrich syndrome causing mutations in the WH1 domain. J Mol Med. 2000; 78(9):530–7. [PubMed: 11140379]

Rottner K, Behrendt B, Small JV, Wehland J. VASP dynamics during lamellipodia protrusion. Nat Cell Biol. 1999; 1(5):321–2. [PubMed: 10559946]

Schirenbeck A, Arasada R, Bretschneider T, Stradal TE, Schleicher M, Faix J. The bundling activity of vasodilator-stimulated phosphoprotein is required for filopodium formation. Proc Natl Acad Sci U S A. 2006; 103(20):7694–9. [PubMed: 16675552]

Smith GA, Theriot JA, Portnoy DA. The tandem repeat domain in the Listeria monocytogenes ActA protein controls the rate of actin-based motility, the percentage of moving bacteria, and the localization of vasodilator-stimulated phosphoprotein and profilin. J Cell Biol. 1996a; 135(3):647–60. [PubMed: 8909540]

Smith JL, Silveira LA, Spudich JA. Activation of Dictyostelium myosin light chain kinase A by phosphorylation of Thr166. Embo J. 1996b; 15(22):6075–83. [PubMed: 8947030]

Smolenski A, Poller W, Walter U, Lohmann SM. Regulation of human endothelial cell focal adhesion sites and migration by cGMP-dependent protein kinase I. J Biol Chem. 2000; 275(33):25723–32. [PubMed: 10851246]

Sun B, Ma H, Firtel RA. Dictyostelium Stress-activated Protein Kinase {alpha}, a Novel Stress-activated Mitogen-activated Protein Kinase Kinase Kinase-like Kinase, Is Important for the Proper Regulation of the Cytoskeleton. Mol Biol Cell. 2003a; 14(11):4526–4540. [PubMed: 14593072]

Sun B, Ma H, Firtel RA. Dictyostelium stress-activated protein kinase alpha, a novel stress-activated mitogen-activated protein kinase kinase kinase-like kinase, is important for the proper regulation of the cytoskeleton. Mol Biol Cell. 2003b; 14(11):4526–40. [PubMed: 14593072]

Svitkina TM, Bulanova EA, Chaga OY, Vignjevic DM, Kojima S, Vasiliev JM, Borisy GG. Mechanism of filopodia initiation by reorganization of a dendritic network. J Cell Biol. 2003; 160(3):409–21. [PubMed: 12566431]

Tokumitsu H, Hatano N, Inuzuka H, Ishikawa Y, Uyeda TQ, Smith JL, Kobayashi R. Regulatory mechanism of Dictyostelium myosin light chain kinase A. J Biol Chem. 2004; 279(1):42–50. [PubMed: 14570871]

Volkman BF, Prehoda KE, Scott JA, Peterson FC, Lim WA. Structure of the N-WASP EVH1 domain-WIP complex: insight into the molecular basis of Wiskott-Aldrich Syndrome. Cell. 2002; 111(4): 565–76. [PubMed: 12437929]

Weber I. Is there a pilot in a pseudopod? Eur J Cell Biol. 2006; 85(9-10):915–24. [PubMed: 16781010]

Wessels D, Lusche DF, Kuhl S, Heid P, Soll DR. PTEN plays a role in the suppression of lateral pseudopod formation during Dictyostelium motility and chemotaxis. J Cell Sci. 2007; 120(15): 2517–2531. [PubMed: 17623773]

Woods A, Vertommen D, Neumann D, Turk R, Bayliss J, Schlattner U, Wallimann T, Carling D, Rider MH. Identification of phosphorylation sites in AMP-activated protein kinase (AMPK) for upstream AMPK kinases and study of their roles by site-directed mutagenesis. J Biol Chem. 2003; 278(31):28434–42. [PubMed: 12764152]

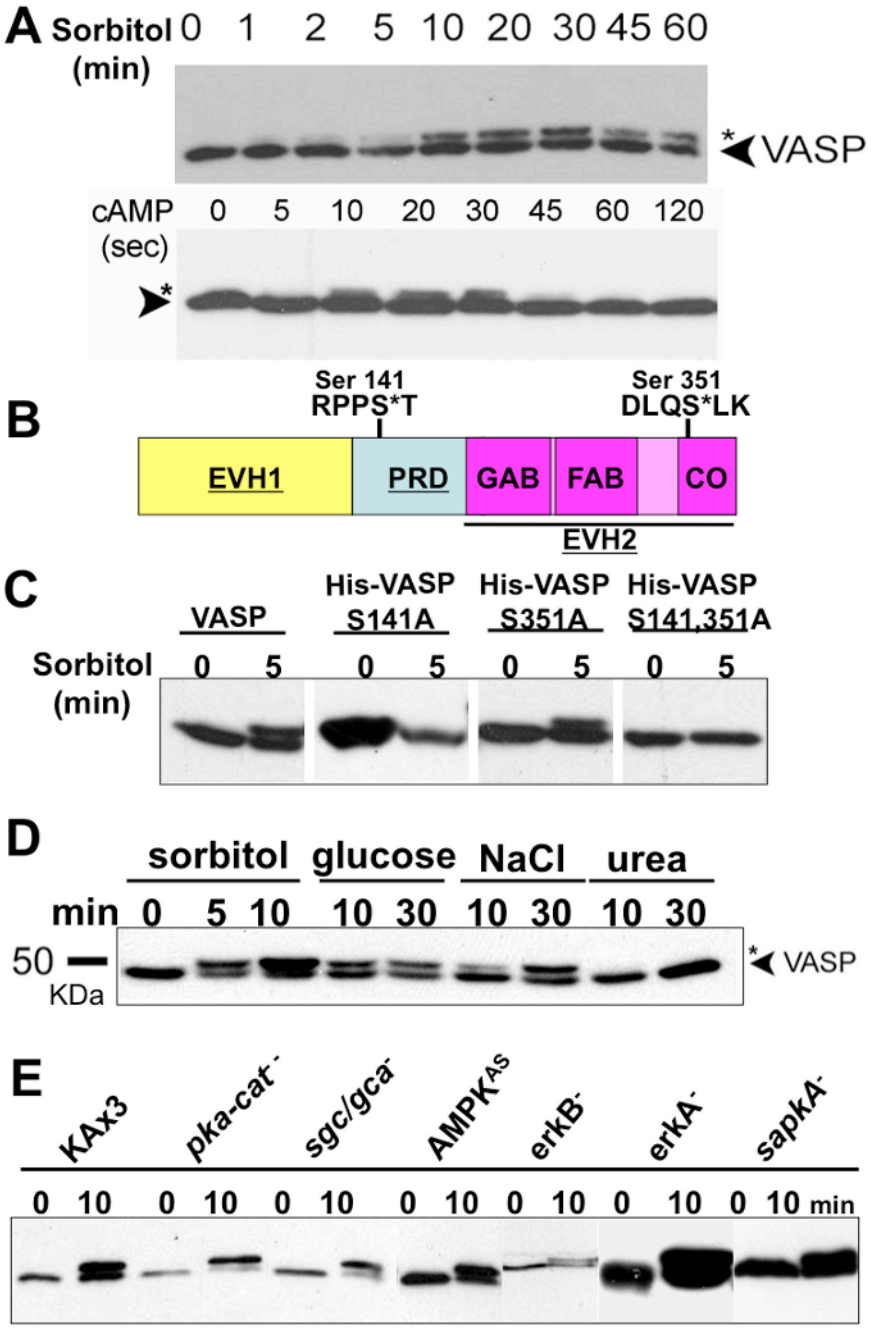

Figure 1. Hyperosmotic stress and extracellular cAMP stimulus induce VASP phosphorylation in a different manner

A, Vegetative and KAx3 cells pulsed 5-hrs (5×10^6/ml) were treated with hyperosmotic shock (0.4M sorbitol, 430 mOsm) and cAMP (100 μM), respectively. Whole cell lysates were taken at different time points as indicated. Samples were subjected to 8% SDS-PAGE and immunoblotting probed with VASP antibody. *B*, Schematic diagram of *Dictyostelium* VASP. PRD (proline-rich domain) is flanked by EVH1((Ena/VASP homology 1) and EVH2 domains. EVH2 domain, indicated with underline, harbors G-actin binding (GAB), F-actin binding (FAB), and coiled-coil (CO) regions. Two putative phosphorylation motifs (Ser-141 and Ser-351) on VASP are shown. *C*, 6× His-tagged VASP phosphorylation mutants

(S141A, S351A, and S141A/S351A) were expressed in *vasp* null background and stimulated with sorbitol. Phosphorylation of VASP was examined by immnoblotting after SDS-PAGE. *D*, Examination of VASP phosphorylation caused by different hyperosmolarity-inducing agents. Cells were exposed to hyperosmotic shock generated by different reagents as indicated for different period of time. *E*, null (*pka-cat*$^{-}$, *sgc/gca*$^{-}$, *erkA*$^{-}$, *erkB*$^{-}$, *sapkA*$^{-}$) and antisense ($AMPK_{AS}$) cells were treated with sorbitol for 10 min. Whole cell lysates were subjected to immunoblotting probed with anti-*Dd*VASP antibody.

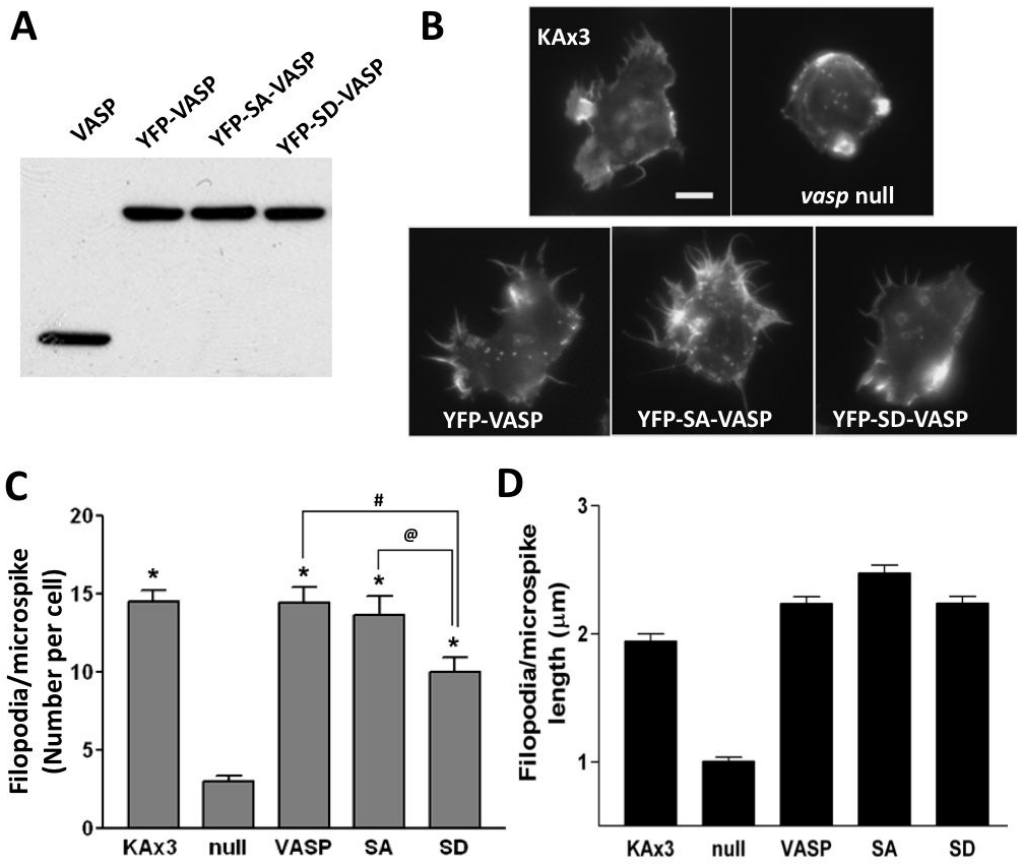

Figure 2. VASP phosphorylation plays a negative role in filopodia/microspikes formation

A, Expression of YFP-tagged VASP mutants in *vasp* null cells. Cells at vegetative stage were lysed and whole cell lysates (30 μg of proteins) were run on SDS-PAGE and subjected to immunoblotting with anti-VASP antibody. Immunoblot shows endogenous (VASP) and exogenous (YFP-VASP) expression. *B*, vegetative cells were synchronized in Na/K phosphate buffer for 30 min followed by permeabilization, fixation and staining with Texas Red-phalloidin. Scale bar represents 5 μm. *C-D*, the number (C) and the length (D) of filopodia/microspikes per cell were counted and presented as a bar graph. Data presented as mean ± SEM. Unpaired Student t-test. (* $p<0.0001$, compared to null cells; # $p<0.01$; @ $p<0.05$)

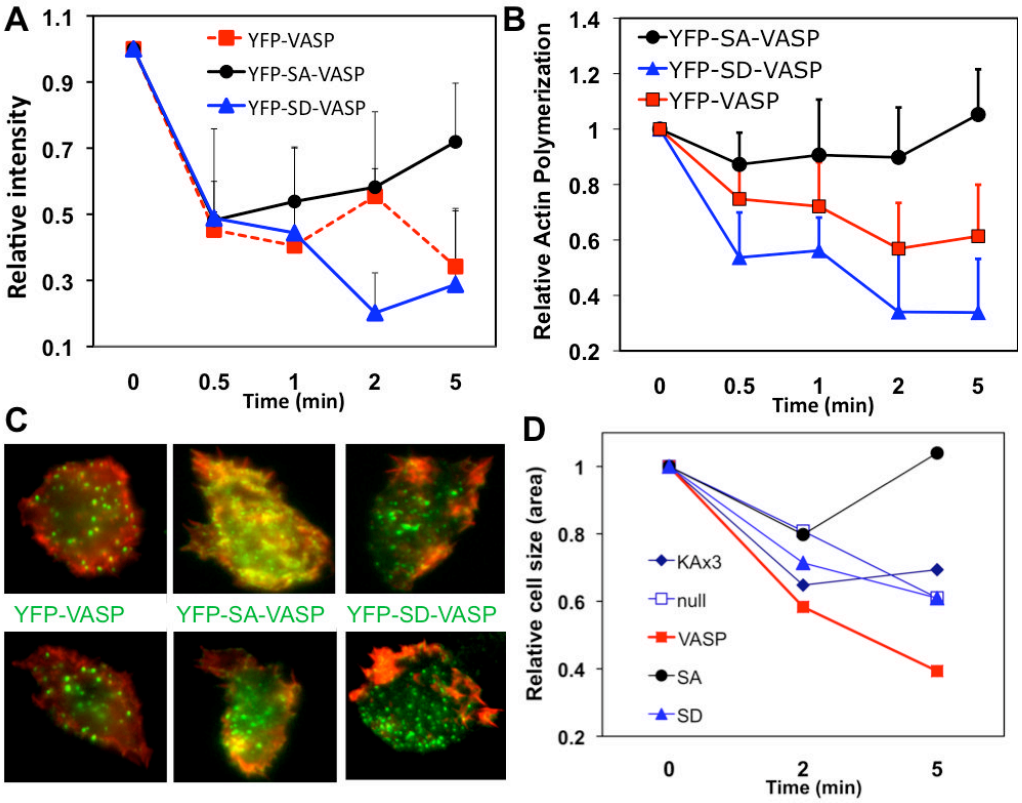

Figure 3. VASP phosphorylation is important for its colocalization with F-actin upon hyperosmotic stress

A, Changes of YFP-VASP associated with a detergent-insoluble fraction. *vasp* null cells expressing YFP-VASP, YFP-S141A (SA)VASP, and YFP-S141D (SD)VASP were treated with 0.2M sorbitol and cells were lysed with lysis buffer at different times. Detergent insoluble fraction (DIF) was prepared by centrifugation of the lysate at 18,00 RPM and run on a PAGE gel. YFP-VASP or mutants associated with the DIF was detected by western blot. Relative band intensity was shown. *B*, Changes of F-actin polymerization in DIF after sorbitol treatment. DIF was run on a PAGE gel and the intensity of actin band was quantified. *C*, Colocalization of VASP or mutants with F-actin after sorbitol treatment. Cells were fixed at 5 min after sorbitol treatment and stained with Texas-Red labeled phalloidin. Images were taken in both YFP (green) and Texas-Red (red) channels and overlaid to show colocalization. *D*, Changes of cell size (area) upon sorbitol treatment. Vegetative cells were synchronized in Na/K phosphate buffer for 30 min followed by 0.2 M sorbitol treatment. Cells were fixed at 2 and 5 min after sorbitol treatment and size of cells was compared to that of untreated controls. Numbers shown are average of minimum 20 measurements. Error bars are not shown to avoid complexity of the graph.

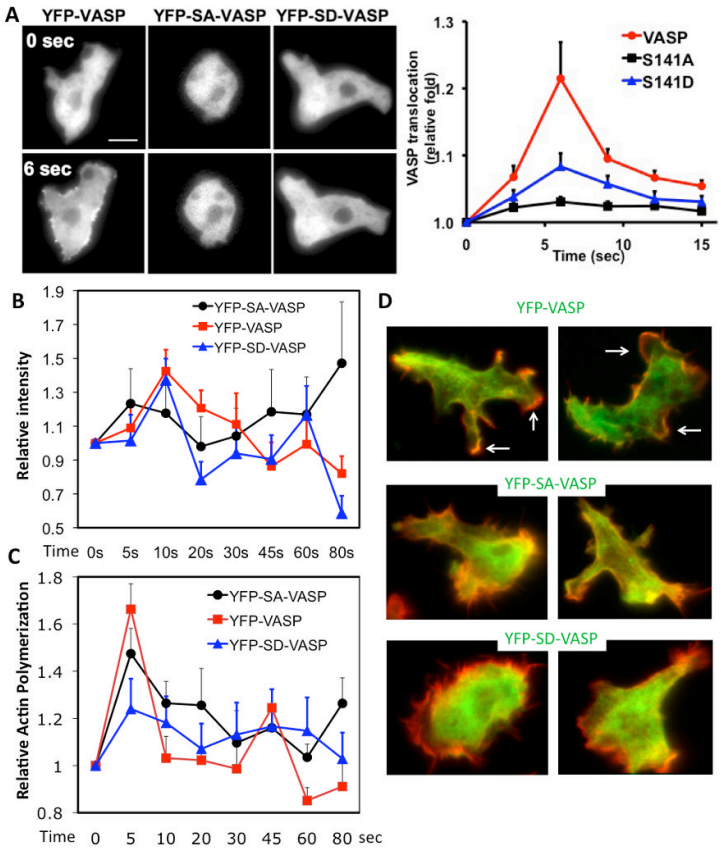

Figure 4. VASP phosphorylation is important for its colocalization with F-actin upon cAMP stimulation

A, Cells (VASP, SA, SD) pulsed for 5-hrs were stimulated uniformly with cAMP (100 nM). Images before (-) and after cAMP stimulus for 6 sec (+) obtained from time-lapse recordings are presented. Right panel shows translocation kinetics of VASP in response to cAMP. Translocation was quantitated using the linescan analysis. Translocation was defined as the ratio of the average pixel intensity at cortex to pixel intensity in the cytosol. 4-6 lines were drawn for individual cells. Data presented as mean ± SEM. The translocation is normalized by 0 time point. Scale bar represents 5 μm. *B*, Association of YFP-VASP into DIF upon cAMP stimulation. DIF was prepared at different time points after cAMP stimulation and YFP-VASP associated with the DIF was detected by western blot. *C*, Changes of F-actin polymerization in DIF after cAMP treatment. *D*, Colocalization of VASP or mutants with F-actin after cAMP stimulation. Cells were fixed at 60 sec after cAMP stimulation and stained with Texas-Red labeled phalloidin. Images were taken in both YFP (green) and Texas-Red (red) channels and overlaid to show colocalization. Arrows indicate pseudopods where VASP and F-actin colocalize.

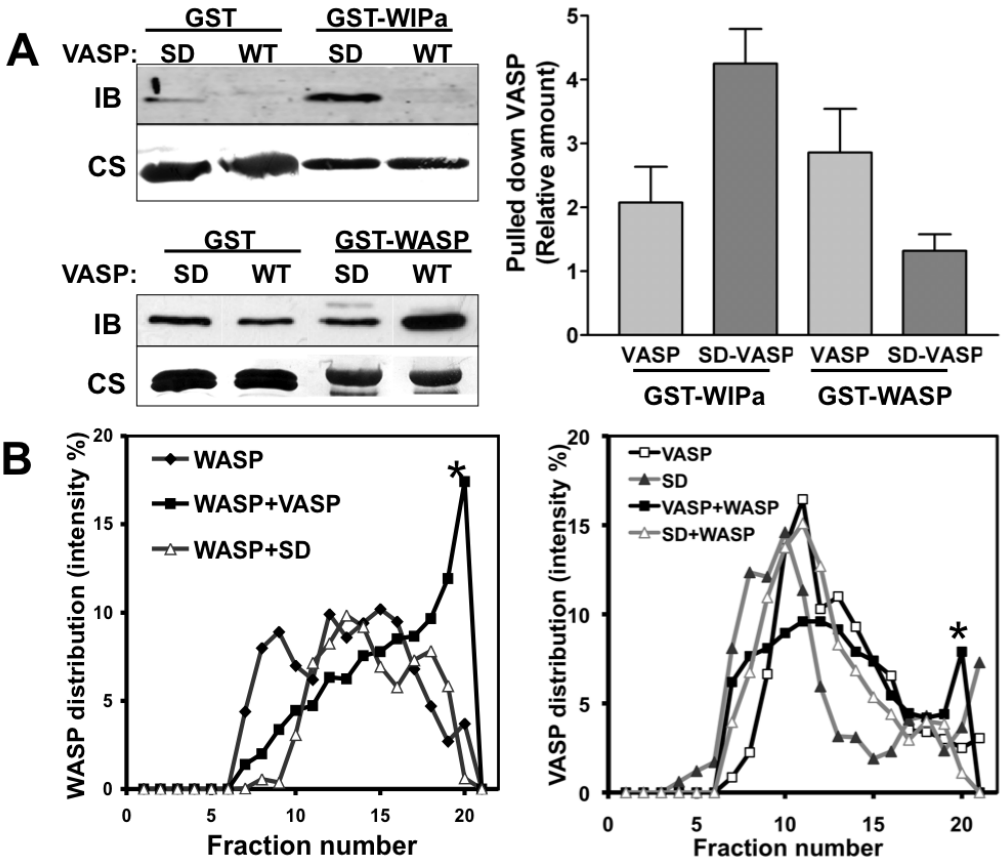

Figure 5. VASP phosphorylation determines the binding affinity to WIPa and WASP

A, Recombinant 6×His-tagged VASP and SD-VASP proteins were precipitated with GST-fusion WIPa and WASP proteins bound to glutathione beads. Samples were subjected to immunoblotting (IB) probed with anti-VASP antibody. The same blot is further stained with Coomassie blue (CS) to visualize GST proteins (left, lower). Band intensities of pulled-down VASP in 3-4 individual experiments were quantitated and normalized to the quantity of GST-tagged protein used in the experiment (right). The pulled down VASP by GST-only beads is considered as 1 in the graph. *B*, Density gradient analysis of the interaction of VASP with WASP. Equal amounts of His-VASP and GST-WASP proteins were preincubated and subjected to ultracentrifugation on an Optiprep gradient (5-20%). Collected fractions were run on a SDS-PAGE gel and stained with Coomassie blue. Relative amounts of His-VASP (~50 kDa, left) and GST-WASP (~ 70 kDa, right) bands from each fraction were quantified and plotted. BSA (~65 kDa) was also run as a protein marker in an additional gradient (5-20%) and is present after fraction 19 (not shown). Stars indicate the GST-WASP (left) or His-VASP (right) or in the higher concentration of Optiprep fractions when VASP and WASP are both present in the reaction.

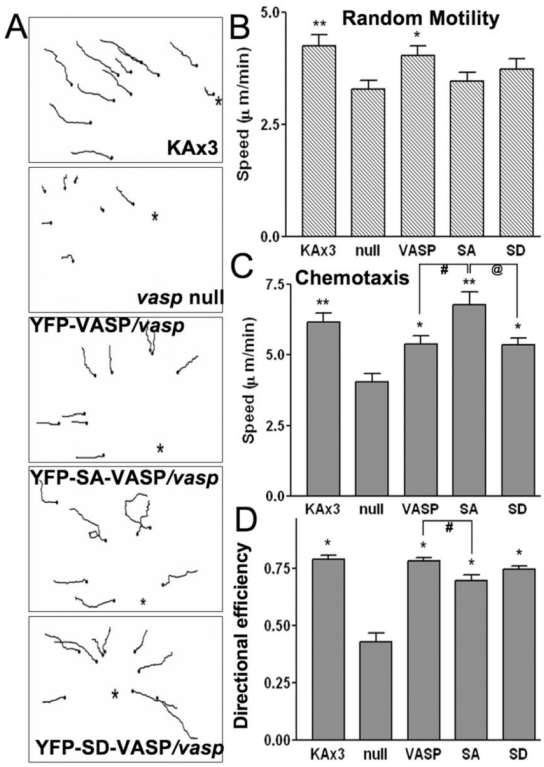

Figure 6.

The role of VASP phosphorylation in random movement and cAMP-driven chemotaxis. *A*, Paths of cell movement from 15 min tracking of chemotaxing cells are shown. Chemotaxis or random movement of aggregation-competent cells were captured using time-lapse microscopy at 3 sec intervals and analyzed with MetaMorph software. Asterisks indicate the direction of the tip of 100 μM cAMP-filled micropipette. *B*, Speed of random motility measured from 2-5 experiments is plotted as a bar graph. (**p<0.01, *p<0.025 compared to null cells.) *C*, Chemotactic movement of cells from 2-4 experiments was analyzed and the speed is shown. Note that unphosphorylated VASP exhibits higher cell speed than VASP and SD cells during chemotaxis. (**p<0.0001, *p<0.01 compared to null cells; #,@ p<0.02). *D*, Effect of VASP phosphorylation on directional efficiency of chemotactic cells. Directional efficiency is defined as the ratio of Euclidean distance (length of direct path) to the actual cell path and plotted as a bar graph. (*p<0.0001 compared to null cells. # p<0.01 by unpaired t-test).

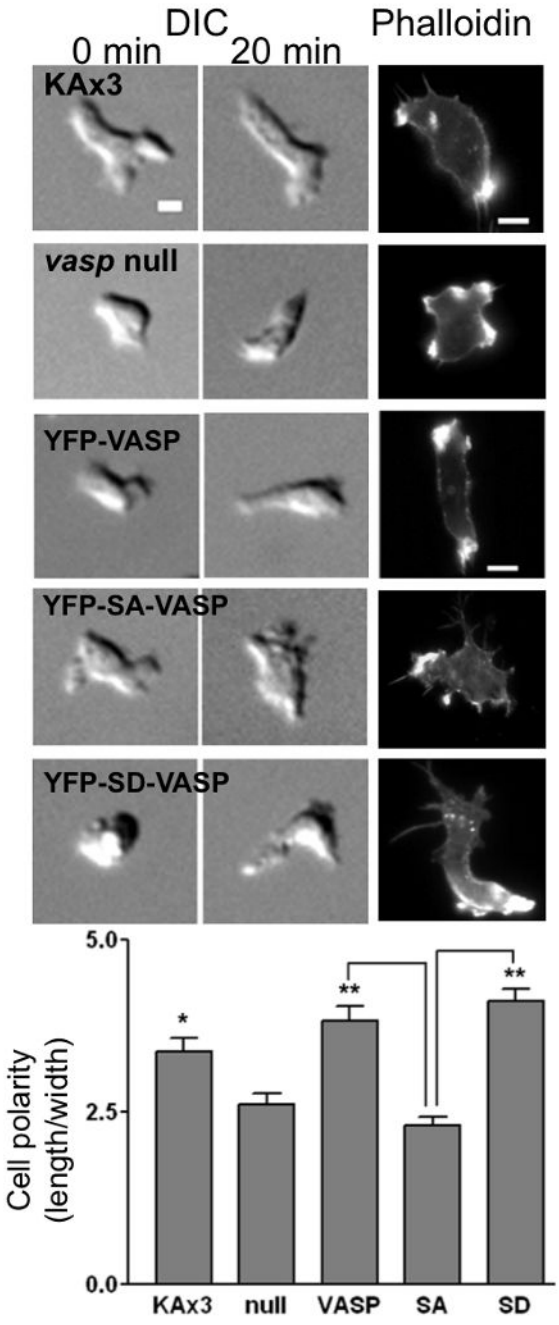

Figure 7. VASP phosphorylation is important for the establishment of cell polarity under cAMP gradient

Representative DIC images of cells before and 20 min after cAMP gradient was established are shown. Scale bar, 5 μm. Phalloidin stainings of chemotaxing cells are also shown. Bottom panel shows axial cell polarity (ratio between length and width of cells in the presence of cAMP gradient) analyzed. Data presented as mean ± SEM. (**p<0.0001, *p<0.01 compared to null cells; # p<0.001)